A Robust and Low-Complexity Walsh-Hadamard Modulation for Doubly-Dispersive Channels

Roberto Bomfin, Ahmad Nimr, Marwa Chafii, Gerhard Fettweis

A Robust and Low-Complexity Walsh-Hadamard Modulation for Doubly-Dispersive Channels

Roberto Bomfin, Ahmad Nimr, Marwa Chafii and Gerhard Fettweis, *Fellow, IEEE*

***Abstract*—In this letter, we present a generic modulation framework for robust wireless communications over doubly dispersive channels. This robustness is achieved by spreading the symbols over time and frequency such that they experience the same channel gain. Interestingly, we show that our modulation framework is a generalization of the recently proposed orthogonal time frequency space modulation (OTFS). By exploiting an additional degree of freedom enabled by the generic framework, we propose in this paper a low-complex waveform based on the sparse Walsh-Hadamard transform (WHT). We show that the proposed sparse WHT modulation exhibits the same frame error rate performance as OTFS, while significantly reducing the implementation complexity due to the multiplication-free small-size WHT compared with the discrete Fourier transform used by symplectic finite Fourier transform (SFFT) of OTFS.**

***Index Terms*—Walsh-Hadamard, MMSE-PIC, doubly dispersive channel, OTFS, OFDM.**

I. Introduction

Achieving reliable and robust wireless communications is essential in future networks for the realization of emerging applications. In order to attain the required end-to-end reliability, the physical layer (PHY) should be robust [1]. However, the wireless channel can be challenging in some applications such as vehicular communications [2], where the channel becomes selective in time and frequency. To overcome the channel's selectivity, several techniques have been considered for frequency-selective channels, which can also be applied to the time-selective case. Among the most common approaches, link adaptation and power loading [3], which require channel state information (CSI) at the transmitter. Without CSI's prior knowledge, another strategy is to design the waveform and employ more advanced iterative receivers such as [4], [5]. However, its computational complexity depends on the underlying modulation scheme.

Modern digital wireless communication systems such as WiFi and 5G rely on the orthogonal frequency division multiplexing (OFDM) modulation, which allows an inter-symbol-interference (ISI)-free separation of the received symbols in pure frequency-selective channel and thus, it enables a simple demodulation. However, it has been shown in [6] that the performance of OFDM is suboptimal in frequency-selective channels. In particular, under the assumption of perfect feedback equalization and no CSI at the transmitter, it is proven that the best modulation should attain the equal gain criterion (EGC) for the data symbols. In practice, the interference cancellation can be realized by means of iterative receivers employing joint decoding and equalization. For instance, a low-complexity minimum mean squared error with parallel interference cancellation (MMSE-PIC) has been used in [4] with orthogonal chirp division multiplexing (OCDM). It is shown that OCDM fulfills the equal-gain criterion, and achieves considerable performance gain over OFDM. Recently, orthogonal time frequency space modulation (OTFS) has been proposed for doubly selective channel [5]. It is shown in [7], that OTFS belongs to a family of precoded OFDM systems, that attain equal signal-to-interference-plus-noise ratio (SINR) after equalization, which, in fact, implies satisfying the EGC.

Motivated by the need for robust wireless communications under distorting channels, the main contribution of this paper is to provide a robust waveform with a low-complexity detection scheme for doubly dispersive wireless channels. Firstly, we present a general modulation framework for doubly dispersive channel providing the required conditions for achieving equal-gain property based on [6]. Secondly, we consider a specific modulation based on the sparse Walsh-Hadamard transform (WHT) that fulfills the EGC and considerably reduces the complexity of the symplectic finite Fourier transform (SFFT) employed by OTFS while achieving the same frame error rate (FER) performance. For the frequency-domain sparsity, we provide a proof for EGC depending on the channel's power delay profile. The time-domain sparsity is considered by analogy and is evaluated numerically. In summary, the proposed low-complexity modulation design is based on two aspects, i) implementing WHT does not require multiplications unlike the discrete Fourier transform (DFT) used in OTFS, and ii) sparse modulation decreases the number of computations without performance loss. For the receiver, we derive a low-complexity LMMSE-PIC similarly to [4].

There is a vast literature about WHT, with several applications, e.g., statistical analysis, signal processing, communications, and more [8]. In wireless communication, the prior works [9], [10] focus on decreasing the uncoded bit error rate (BER), and [11] considers only the time invariant channel, whereas [12] studies a full spreading waveform. In this letter, we generalize the scheme studied in [12] by proposing a sparse waveform with decreased complexity.

Notations: Vectors and matrices are denoted as $\boldsymbol{a}$, $\boldsymbol{A}$, respectively. The n-th element of a vector is $\boldsymbol{a}[n]$, the (k,m)-th element in a matrix is denoted as $\boldsymbol{A}[k,m]$, and the m-th row as $\boldsymbol{A}[:,m]$. For $\boldsymbol{A}$ being a $N \times N$ matrix, the operator

R. Bomfin, A. Nimr and G. Fettweis are with the Vodafone Chair Mobile Communications Systems, Technische Universität Dresden, 01187 Dresden, Germany (e-mail: roberto.bomfin@ifn.et.tu-dresden.de; ahmad.nimr@ifn.et.tu-dresden.de;gerhard.fettweis@tu-dresden.de). M. Chafii is with ETIS, UMR 8051, CY Paris Université, ENSEA, CNRS, 95000 Cergy, France (e-mail: marwa.chafii@ensea.fr). This project has received funding from the European Union's Horizon 2020 research and innovation programme through the project iNGENIOUS under grant agreement No 957216, and the CY Initiative of Excellence through the ASIA Chair of Excellence Grant (PIA/ANR-16-IDEX-0008).

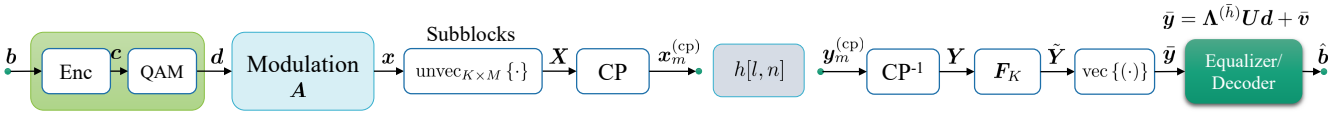

Fig. 1: Generic block modulation.

$\text{diag}\{\boldsymbol{A}\}$ returns a column vector of size N with elements taken from the diagonal of $\boldsymbol{A}$. The operator $\text{trace}\{\boldsymbol{A}\}$ returns the trace of $\boldsymbol{A}$. Let $\boldsymbol{a}$ and $\boldsymbol{b}$ be column vectors of size N, $\boldsymbol{c} = \boldsymbol{a}/\boldsymbol{b}$ is an N size column vector and corresponds to an element-wise of $\boldsymbol{a}$ by $\boldsymbol{b}$. The vectorization of a matrix according to the columns is expressed as $\boldsymbol{a} = \text{vec}\{\boldsymbol{A}\}$. The inverse of vectorization, which constructs a matrix of size $K \times M$ is written as $\boldsymbol{A} = \text{unvec}_{K\times M}\{\boldsymbol{a}\}$. The matrices $\boldsymbol{I}_N$ and $\boldsymbol{F}_N$ refer to the $N \times N$ identity and normalized N-DFT matrices, respectively. The vectors $\boldsymbol{0}_N$, and $\boldsymbol{1}_N$ denote the all zeros and all ones column vectors of size N, respectively. The operator $\mathbb{E}[\cdot]$ denotes expectation, $\odot$ element-wise product, $\otimes$ Kronecker product, $(\cdot)^{\text{T}}$ transpose, $(\cdot)^{\text{H}}$ Hermitian transpose, and $\langle\cdot\rangle_N$ modulo-N operator.

II. Generic block modulation framework

Consider a generic linear modulation, where a modulated block $\boldsymbol{x} \in \mathbb{C}^{N\times 1}$ is generated using a matrix $\boldsymbol{A} \in \mathbb{C}^{N\times N}$ as $\boldsymbol{x} = \boldsymbol{A}\boldsymbol{d}$, $\boldsymbol{d} \in \mathcal{S}^{N\times 1}$ denotes the vector of data symbols whose elements are selected from the quadurature amplitude modulation (QAM) constellation set $\mathcal{S}$, with cardinality $|\mathcal{S}| = J$. These symbols are generated by the mapping of the interleaved encoded bits denoted as $\boldsymbol{c}$, which corresponds to data bits $\boldsymbol{b}$. The elements of $\boldsymbol{d}$ are assumed to be uncorrelated with equal power E_s, such that $\mathbb{E}[\boldsymbol{d}\boldsymbol{d}^{\text{H}}] = E_s\boldsymbol{I}_N$. Assuming a linear time-variant (LTV) channel defined by the impulse response $h[l,n]$, with a coherence time sufficiently smaller than the time required to transmit K samples such that $h[l,k+mK] \approx h[l,m], k = 0\cdots K-1$. Accordingly, $\boldsymbol{x}$ is split into M sub-blocks defined by $\boldsymbol{X} = [\boldsymbol{x}_0,\cdots,\boldsymbol{x}_{M-1}] = \text{unvec}_{K\times M}\{\boldsymbol{x}\}$, where $N = MK$ and $\boldsymbol{x}_m \in \mathbb{C}^{K\times 1}$. Considering $L << K$ delay taps of the channel, a cyclic prefix (CP) of length $K_{\text{cp}} \geq L-1$ samples is appended per sub-block to get $\boldsymbol{x}_m^{(\text{cp})}$.

A. Received signal model

Assuming that the channel is static during the transmission of a sub-block, the m-th received sub-block after removing the CP from $\boldsymbol{y}_m^{(\text{cp})}$ can be expressed as

$$\boldsymbol{y}_m = \boldsymbol{H}_m\boldsymbol{x}_m + \boldsymbol{v}_m. \tag{1}$$

Here $\boldsymbol{H}_m \in \mathbb{C}^{K\times K}$, $\boldsymbol{H}_m[k,q] = h_m[\langle k-q\rangle_K]$ is the circular channel matrix associated with the m-th sub-block, and $\boldsymbol{v}_m \in \mathbb{C}^{K\times 1}$ is additive white Gaussian noise (AWGN) with power N_0, such that $\text{E}\left[\boldsymbol{v}_{m_1}\boldsymbol{v}_{m_2}^{\text{H}}\right] = N_0\boldsymbol{I}_K$, when $m_1 = m_2$ and $\boldsymbol{0}_K$ otherwise. The respective frequency domain (FD) signal is obtained using K-DFT,

$$\tilde{\boldsymbol{y}}_m = \tilde{\boldsymbol{h}}_m \odot \tilde{\boldsymbol{x}}_m + \tilde{\boldsymbol{v}}_m, \tag{2}$$

where, $\tilde{\boldsymbol{y}}_m = \boldsymbol{F}_K\boldsymbol{y}_m$, and $\tilde{\boldsymbol{h}}_m = \boldsymbol{F}_K\boldsymbol{H}_m[:,1]$. By stacking the vectors of (2) in a matrix of size $K \times M$, defined as $\tilde{\boldsymbol{Y}} = [\tilde{\boldsymbol{y}}_0,\cdots,\tilde{\boldsymbol{y}}_{M-1}]$, and let $\boldsymbol{Y} = [\boldsymbol{y}_0,\cdots,\boldsymbol{y}_{M-1}]$, $\tilde{\boldsymbol{H}} = [\tilde{\boldsymbol{h}}_0,\cdots,\tilde{\boldsymbol{h}}_{M-1}]$, $\tilde{\boldsymbol{X}} = [\tilde{\boldsymbol{x}}_0,\cdots,\tilde{\boldsymbol{x}}_{M-1}]$, and $\tilde{\boldsymbol{V}} = [\tilde{\boldsymbol{v}}_0,\cdots,\tilde{\boldsymbol{v}}_{M-1}]$, then all received sub-blocks can be expressed in the following compact form

$$\tilde{\boldsymbol{Y}} = \tilde{\boldsymbol{H}} \odot \tilde{\boldsymbol{X}} + \tilde{\boldsymbol{V}} \Rightarrow \boldsymbol{F}_K\boldsymbol{Y} = \tilde{\boldsymbol{H}} \odot [\boldsymbol{F}_K\boldsymbol{X}] + \tilde{\boldsymbol{V}}. \tag{3}$$

Applying the vectorization operation to (3) and combining $\text{vec}\{\boldsymbol{F}_K\boldsymbol{X}\} = (\boldsymbol{I}_M \otimes \boldsymbol{F}_K)\,\boldsymbol{x}$ with $\boldsymbol{x} = \boldsymbol{A}\boldsymbol{d}$, we get

$$\bar{\boldsymbol{y}} = \text{vec}\left\{\tilde{\boldsymbol{Y}}\right\} = \boldsymbol{\Lambda}^{(h)}\,(\boldsymbol{I}_M \otimes \boldsymbol{F}_K)\,\boldsymbol{A}\boldsymbol{d} + \bar{\boldsymbol{v}},$$

where $\boldsymbol{\Lambda}^{(h)} = \text{diag}\left\{\text{vec}\left\{\tilde{\boldsymbol{H}}\right\}\right\}$ represents the FD block channel matrix. The matrix $\bar{\boldsymbol{A}} = (\boldsymbol{I}_M \otimes \boldsymbol{F}_K)\,\boldsymbol{A}$ corresponds to the FD block modulation matrix. To simplify the equalization, $\bar{\boldsymbol{A}}$ can be designed using unitary transform whose matrix is $\boldsymbol{U}$, with $\boldsymbol{U}\boldsymbol{U}^{\text{H}} = \boldsymbol{I}_N$, and a diagonal matrix $\boldsymbol{\Lambda}^{(\text{tx})}$ which performs FD windowing, such that $\bar{\boldsymbol{A}} = \boldsymbol{\Lambda}^{(\text{tx})}\boldsymbol{U}$. Accordingly,

$$\boldsymbol{A} = \left(\boldsymbol{I}_M \otimes \boldsymbol{F}_K^{\text{H}}\right)\boldsymbol{\Lambda}^{(\text{tx})}\boldsymbol{U}. \tag{4}$$

As a result, using the equivalent channel $\boldsymbol{\Lambda}^{(\bar{h})} = \boldsymbol{\Lambda}^{(h)}\boldsymbol{\Lambda}^{(\text{tx})}$, the received signal can be written as

$$\bar{\boldsymbol{y}} = \boldsymbol{\Lambda}^{(\bar{h})}\boldsymbol{U}\boldsymbol{d} + \bar{\boldsymbol{v}}. \tag{5}$$

B. Relation to OFDM precoding

Using the special case (4), the modulated block can be expressed as $\boldsymbol{x} = \left(\boldsymbol{I}_M \otimes \boldsymbol{F}_K^{\text{H}}\right)\boldsymbol{\Lambda}^{(\text{tx})}\boldsymbol{U}\boldsymbol{d}$, which means, that the modulation is performed in 3 steps; 1) unitary precoding of the data $\boldsymbol{d}_{\text{p}} = \boldsymbol{U}\boldsymbol{d}$, 2) windowing with $\boldsymbol{d}_{\text{p,w}} = \boldsymbol{\Lambda}^{(\text{tx})}\boldsymbol{d}_{\text{p}}$, and 3) block OFDM modulation. For special precoding design given by $\boldsymbol{U} = (\boldsymbol{U}_M \otimes \boldsymbol{U}_K)$, where $\boldsymbol{U}_M \in \mathbb{C}^{M\times M}$ and $\boldsymbol{U}_M \in \mathbb{C}^{K\times K}$ are unitary matrices, the sub-block matrix $\boldsymbol{X}$ can be expressed as

$$\boldsymbol{X} = \boldsymbol{F}_K^{\text{H}}\left(\boldsymbol{G}^{(\text{tx})} \odot \left[\boldsymbol{U}_K\boldsymbol{D}\boldsymbol{U}_M^{\text{T}}\right]\right) = \boldsymbol{F}_K^{\text{H}}\boldsymbol{D}_{\text{p,w}}. \tag{6}$$

where $\boldsymbol{D} = \text{unvec}_{K\times M}\{\boldsymbol{d}\}$, $\boldsymbol{G} \in \mathbb{C}^{K\times M}$ is defined such as $\boldsymbol{\Lambda}^{(\text{tx})} = \text{diag}\{\text{vec}\{\boldsymbol{G}\}\}$, and $\boldsymbol{D}_{\text{p,w}} = \boldsymbol{G} \odot [\boldsymbol{U}_K\boldsymbol{D}\boldsymbol{U}_M]$ denotes precoded data symbols. The system model is equivalent to transmitting M CP-OFDM symbols with K subcarriers modulated by the precoded data $\boldsymbol{D}_{\text{p,w}}$. This framework is more general than the one introduced in [13]. As particular cases of precoding on top of OFDM, OTFS employs $(\boldsymbol{F}_M^H, \boldsymbol{F}_K)$, block-single carrier (SC), where the sub-blocks are given by $\boldsymbol{x}_m = \boldsymbol{D}[:,m]$ use $(\boldsymbol{I}_M, \boldsymbol{F}_K)$. In this letter, the sparse Walsh-Hadamard (WH) precoding is proposed with $\boldsymbol{U}_K = \boldsymbol{W}_Q \otimes \boldsymbol{I}_P$ and $\boldsymbol{U}_M = \boldsymbol{W}_{Q'} \otimes \boldsymbol{I}_{P'}$, where $\boldsymbol{W}_N$ denotes, the normalized WHT matrix defined recursively by

$$\boldsymbol{W}_N = \boldsymbol{W}_2 \otimes \boldsymbol{W}_{N/2},\ \boldsymbol{W}_2 = \frac{1}{\sqrt{2}}\begin{bmatrix} 1 & 1 \\ 1 & -1 \end{bmatrix}. \tag{7}$$

More details on this precoding are presented in Section III.

C. Iterative Equalizer

Depending on the modulation matrix, an iterative equalization is necessary to resolve the ISI caused by the dispersive wireless channel. The MMSE-PIC [4] is adopted in this work. For the received signal (5), the general MMSE-PIC is computed as

$$\hat{\boldsymbol{d}} = \boldsymbol{d}^{\mathrm{a}} + \frac{\boldsymbol{U}^{\mathrm{H}}\boldsymbol{\Lambda}^{(\bar{h})^{\mathrm{H}}}\left(\boldsymbol{\Lambda}^{(\bar{h})}\boldsymbol{U}\boldsymbol{\Sigma}^{\mathrm{a}}_{\boldsymbol{d}}\boldsymbol{U}^{\mathrm{H}}\boldsymbol{\Lambda}^{(\bar{h})^{\mathrm{H}}}+\boldsymbol{I}N_0\right)^{-1}\left(\bar{\boldsymbol{y}}-\boldsymbol{\Lambda}^{(\bar{h})}\boldsymbol{U}\boldsymbol{d}^{\mathrm{a}}\right)}{\mathrm{diag}\left\{\boldsymbol{U}^{\mathrm{H}}\boldsymbol{\Lambda}^{(\bar{h})^{\mathrm{H}}}\left(\boldsymbol{\Lambda}^{(\bar{h})}\boldsymbol{U}\boldsymbol{\Sigma}^{\mathrm{a}}_{\boldsymbol{d}}\boldsymbol{U}^{\mathrm{H}}\boldsymbol{\Lambda}^{(\bar{h})^{\mathrm{H}}}+\boldsymbol{I}N_0\right)^{-1}\boldsymbol{\Lambda}^{(\bar{h})}\boldsymbol{U}\right\}} \quad (8)$$

and[1]

$$\boldsymbol{\Sigma}_{\hat{\boldsymbol{d}}} = \frac{\mathbf{1}_N}{\mathrm{diag}\left\{\boldsymbol{U}^{\mathrm{H}}\boldsymbol{\Lambda}^{(\bar{h})^{\mathrm{H}}}\left(\boldsymbol{\Lambda}^{(\bar{h})}\boldsymbol{U}\boldsymbol{\Sigma}^{\mathrm{a}}_{\boldsymbol{d}}\boldsymbol{U}^{\mathrm{H}}\boldsymbol{\Lambda}^{(\bar{h})^{\mathrm{H}}}+\boldsymbol{I}N_0\right)^{-1}\boldsymbol{\Lambda}^{(\bar{h})}\boldsymbol{U}\right\} - \mathrm{diag}\left\{\boldsymbol{\Sigma}^{\mathrm{a}}_{\boldsymbol{d}}\right\}} \quad (9)$$

where $\hat{\boldsymbol{d}} \in \mathbb{C}^{N\times 1}$ is the estimated data symbol and $\boldsymbol{\Sigma}_{\hat{\boldsymbol{d}}} \in \mathbb{C}^{N\times 1}$ is the error variance of the estimated data. In addition, $\boldsymbol{d}^{\mathrm{a}} \in \mathbb{C}^{N\times 1}$ and $\boldsymbol{\Sigma}^{\mathrm{a}}_{\boldsymbol{d}} \in \mathbb{C}^{N\times N}$ are the a-priori data mean and the diagonal error variance matrix, respectively, which are computed based on the log likelihood ratios (LLRs) produced by the single-input single-output (SISO) decoder, e.g., BCJR log-MAP. In this letter, the computation of $\boldsymbol{d}^{\mathrm{a}}$ and $\boldsymbol{\Sigma}^{\mathrm{a}}_{\boldsymbol{d}}$ is omitted for brevity, and can be found in detail in [14, eq. (13)]. At the initial step, these variables are $\boldsymbol{d}^{\mathrm{a}} = \mathbf{0}_N$ and $\boldsymbol{\Sigma}^{\mathrm{a}}_{\boldsymbol{d}}[n,n'] = 1$ for $n = n'$ and 0 otherwise.

III. Robust and Low-Complexity Modulation

A. Sparse Walsh-Hadamard (SWH)

1) Frequency Domain Sparsity: As opposed to [6], in the following we show that the EGC can be achieved with sparse spreading in order to reduce the computational complexity. Omitting the index m for simplicity, the received signal (1) is $\boldsymbol{y} = \boldsymbol{H}\boldsymbol{A}\boldsymbol{d} + \boldsymbol{v}$, where $\boldsymbol{x}_m$ is replaced by the modulated data $\boldsymbol{A}\boldsymbol{d}$. Now, Consider the sparse Walsh-Hadamard modulation matrix in time domain $\boldsymbol{A}_{\mathrm{SWH}} = \boldsymbol{W}_P \otimes \boldsymbol{I}_Q$, where $P \cdot Q = K$ and $Q \geq L$. For the first column $\boldsymbol{A}_{\mathrm{SWH}}[0,:] = 1/\sqrt{P}\left(1, \mathbf{0}^{\mathrm{T}}_{Q-1}, 1, \mathbf{0}^{\mathrm{T}}_{Q-1}, \cdots, 1, \mathbf{0}^{\mathrm{T}}_{Q-1}\right)^{\mathrm{T}}$, we can prove that the EGC [6] is achieved by the equality

$$\sum_{n'=0}^{K-1} |(\boldsymbol{H}\boldsymbol{A}_{\mathrm{SWH}})[0,n']|^2 = \sum_{n'=0}^{K-1} |\boldsymbol{H}[0,n']|^2. \quad (10)$$

Next we show that (10) holds. While $Q \geq L$, one can verify that this waveform convoluted with the wireless channel has an output equal to $\boldsymbol{H}\boldsymbol{A}_{\mathrm{SWH}}[0,:] = 1/\sqrt{P}\left(\boldsymbol{h}^{\mathrm{T}}, \mathbf{0}^{\mathrm{T}}_{Q-L}, \boldsymbol{h}^{\mathrm{T}}, \mathbf{0}^{\mathrm{T}}_{Q-L}, \cdots, \boldsymbol{h}^{\mathrm{T}}, \mathbf{0}^{\mathrm{T}}_{Q-L}\right)^{\mathrm{T}}$, where $\boldsymbol{h} \in \mathbb{C}^L$ is the channel impulse response, i.e., the first L elements of the first column of $\boldsymbol{H}$. Clearly, $\boldsymbol{H}\boldsymbol{A}_{\mathrm{SWH}}[0,:]$ appends the channel response P times and multiplies by a factor of $1/\sqrt{P}$. Therefore, it can be easily validated that equation (10) holds. Conversely if $Q < L$, $\boldsymbol{H}\boldsymbol{A}_{\mathrm{SWH}}[0,:]$ cannot be written as above because the channel's coefficients superpose, thus (10) is not guaranteed to hold.

In the frequency domain, we have[2] $\boldsymbol{F}_K\boldsymbol{A}_{\mathrm{SWH}}[0,:] = 1/\sqrt{Q}\left(1, \mathbf{0}^{\mathrm{T}}_{P-1}, 1, \mathbf{0}^{\mathrm{T}}_{P-1}, \cdots, 1, \mathbf{0}^{\mathrm{T}}_{P-1}\right)^{\mathrm{T}}$, where Q and P are swapped. We can make two observations, i) any cyclic shift of $\boldsymbol{F}_K\boldsymbol{A}_{\mathrm{SWH}}[0,:]$ still maintains the ECG of (10) because in the time domain it results in an element wise product with $\boldsymbol{A}_{\mathrm{SWH}}[0,:]$ which does not change the received power, and ii) any phase change in the amplitude of $\boldsymbol{F}_K\boldsymbol{A}_{\mathrm{SWH}}[0,:]$ also maintains the ECG of (10). Thus, the SWH modulation in the frequency domain $\boldsymbol{U}_{\mathrm{SWH}} = \boldsymbol{W}_Q \otimes \boldsymbol{I}_P$ guarantees the ECG.

In summary, we have proved that for a channel impulse response with length L, we can sparsely spread the symbols in FD by an interval of P samples with $P \cdot Q = K$ and $Q \geq L$.

2) Time Domain (sub-block) Sparsity: Analogously to the previous findings with $M = 1$, we generalize the sparse WH modulation for any M. To this end, we make $\boldsymbol{U}_M = \boldsymbol{W}_{Q'} \otimes \boldsymbol{I}_{P'}$ in Subsection II-B such that the data symbols are sparsely spread among the sub-blocks, with $Q' \cdot P' = M$. Basically, if the channel among the sub-blocks are highly correlated, the sparse spreading over the sub-blocks have similar effect as the respective frequency domain sparse spreading. This behavior we will numerically evaluated in Section IV.

Thus, the general sparse Walsh-Hadamard transform for doubly dispersive channels is given as

$$\boldsymbol{U}_{\mathrm{SWH}} = (\boldsymbol{W}_{Q'} \otimes \boldsymbol{I}_{P'}) \otimes (\boldsymbol{W}_Q \otimes \boldsymbol{I}_P). \quad (11)$$

We note that (11) is more general than the one presented in [12], which has $Q = K$ and $Q' = M$, i.e., full spreading.

B. Low-complexity equalization

In order to avoid the N-size matrix inversion of equations (8) and (9) as done in [4], we consider only the diagonal of $\boldsymbol{U}\boldsymbol{\Sigma}^{\mathrm{a}}_{\boldsymbol{d}}\boldsymbol{U}^{\mathrm{H}}$ that according to Appendix is computed as

$$\boldsymbol{\Sigma}^{\mathrm{a}}_{\boldsymbol{X}}[n,n] = \frac{1}{|\chi(n)|}\sum_{n'\in\chi(n)} \boldsymbol{\Sigma}^{\mathrm{a}}_{\boldsymbol{d}}[n',n'], \quad (12)$$

for $n = 0, 1, \cdots, N-1$, where the set $\chi(n) = \{n' | n' \text{ is an index, and } \boldsymbol{U}[n,n'] \neq 0\}$ contains the indexes of the data allocated in the n-th data symbol. Then, this matrix inversion of (8) can be approximated as $\left(\boldsymbol{\Lambda}^{(\bar{h})}\boldsymbol{U}\boldsymbol{\Sigma}^{\mathrm{a}}_{\boldsymbol{d}}\boldsymbol{U}^{\mathrm{H}}\boldsymbol{\Lambda}^{(\bar{h})^{\mathrm{H}}}+\boldsymbol{I}\sigma^2\right)^{-1} \approx \left(\boldsymbol{\Lambda}^{(\bar{h})}\boldsymbol{\Sigma}^{\mathrm{a}}_{\boldsymbol{X}}\boldsymbol{\Lambda}^{(\bar{h})^{\mathrm{H}}}+\boldsymbol{I}\sigma^2\right)^{-1}$, which can be realized with element-wise multiplication.

In addition, we can compute the denominator of (8) analogously to (12) because they have the exact format. Consider the diagonal $\boldsymbol{\Lambda}_{\mathrm{eq}} = \boldsymbol{\Lambda}^{(\bar{h})^{\mathrm{H}}}\left(\boldsymbol{\Lambda}^{(\bar{h})}\boldsymbol{\Sigma}^{\mathrm{a}}_{\boldsymbol{X}}\boldsymbol{\Lambda}^{(\bar{h})^{\mathrm{H}}}+N_0\boldsymbol{I}_N\right)^{-1}\boldsymbol{\Lambda}^{(\bar{h})}$, and because $\boldsymbol{U}$ and $\boldsymbol{U}^{\mathrm{H}}$ have non zero elements in the same position, we have

$$\bar{\boldsymbol{\Lambda}}_{\mathrm{eq}}[n,n] = (\boldsymbol{U}^{\mathrm{H}}\boldsymbol{\Lambda}_{\mathrm{eq}}\boldsymbol{U})[n,n] = \frac{1}{|\chi(n)|}\sum_{n'\in\chi(n)} \boldsymbol{\Lambda}_{\mathrm{eq}}[n',n']. \quad (13)$$

Finally, the low-complexity equalizer for a generic spreading modulation matrix is given by

$$\hat{\boldsymbol{d}} = \boldsymbol{d}^{\mathrm{a}} + \frac{1}{\bar{\boldsymbol{\Lambda}}_{\mathrm{eq}}}\boldsymbol{U}^{\mathrm{H}}\boldsymbol{\Lambda}^{(\bar{h})^{\mathrm{H}}}\left(\boldsymbol{\Lambda}^{(\bar{h})}\boldsymbol{\Sigma}^{\mathrm{a}}_{\boldsymbol{X}}\boldsymbol{\Lambda}^{(\bar{h})^{\mathrm{H}}}+\boldsymbol{I}\sigma^2\right)^{-1}\left(\bar{\boldsymbol{y}}-\boldsymbol{\Lambda}^{(\bar{h})}\boldsymbol{U}\boldsymbol{d}^{\mathrm{a}}\right) \quad (14)$$

[1]Following the notation of [4], we define $\boldsymbol{\Sigma}_{\hat{\boldsymbol{d}}}$ as a vector to keep the notation cleaner.

[2]The DFT of a Dirac comb signal is also a Dirac comb signal.

TABLE I: Complexity of $\boldsymbol{U}$.

	$\boldsymbol{U}$	Multiplications	Additions
SC	$\boldsymbol{I}_M \otimes \boldsymbol{F}_K$	$N/2\log_2(K)$	$N\log_2(K)$
OTFS	$\boldsymbol{F}_M^{\mathrm{H}} \otimes \boldsymbol{F}_K$	$N/2\log_2(N)$	$N\log_2(N)$
SWH	$(\boldsymbol{W}_{Q'} \otimes \boldsymbol{I}_{P'})$ $\otimes (\boldsymbol{W}_Q \otimes \boldsymbol{I}_P)$	N, $\sqrt{QQ'}$ not radix-2 0, $\sqrt{QQ'}$ radix-2	$N\log_2(QQ')$

$$\text{and} \qquad \boldsymbol{\Sigma}_{\hat{\boldsymbol{d}}}[n] = \frac{1}{\bar{\boldsymbol{\Lambda}}_{\mathrm{eq}}} - \boldsymbol{\Sigma}^{\mathrm{a}}_{\boldsymbol{X}}. \tag{15}$$

For the OTFS modulation, (14) and (15) still hold. In this case, the set $\chi(n) = \{0, 1, \cdots, N-1\}\,\forall_n$ in (12) and (13) contains all indexes because the symbols are equally spread over frequency and sub-blocks. Finally, for the SC modulation, $\chi(n) = \{iK, iK+1, \cdots, K+iK-1\}$, where $i = \lfloor nK \rfloor$.

C. Precoding Computational complexity

Table I summarizes the precoding complexity considering for SC, OTFS and SWH. We do not consider OFDM because it has no precoding, i.e., $\boldsymbol{U} = \boldsymbol{I}$. For the SC (DFT-precoding), $\boldsymbol{U} = \boldsymbol{I}_M \otimes \boldsymbol{F}_K$ requires M times K-sized FFT, where the K-sized FFT requires $K/2\log_2(K)$ multiplications and $K\log_2(K)$ additions. In Table I, we make $N = MK$. For OTFS, the precoder is $\boldsymbol{U} = \boldsymbol{F}_M^{\mathrm{H}} \otimes \boldsymbol{F}_K$ whose complexity is equivalent to N-sized FFT [5], i.e., $N/2\log_2(N)$ multiplications and $N\log_2(N)$ additions.

For the proposed SWH in (11), the complexity is computed as follows. Consider $\boldsymbol{U}_{\mathrm{SWH}} = \boldsymbol{U}_M \otimes \boldsymbol{U}_K$ as in Subsection II-B, where according to (11) we make $\boldsymbol{U}_K = \boldsymbol{W}_Q \otimes \boldsymbol{I}_P$ and $\boldsymbol{U}_M = \boldsymbol{W}_{Q'} \otimes \boldsymbol{I}_{P'}$. Then, we write $\boldsymbol{U}_{\mathrm{SWH}}\boldsymbol{d}$ as $\mathrm{vec}\left\{\boldsymbol{U}_K \boldsymbol{D} \boldsymbol{U}_M^{\mathrm{T}}\right\}$, where $\boldsymbol{D} \in \mathcal{S}^{K\times M}$ is the data matrix. The transform $\tilde{\boldsymbol{D}} = \boldsymbol{U}_K\boldsymbol{D}$ consumes a Q-sized FWHT $P \cdot M$ times, where P comes from $\boldsymbol{I}_P$ and M is because $\boldsymbol{D}$ has M columns. Then, the remaining transform $(\boldsymbol{U}_M\tilde{\boldsymbol{D}}^{\mathrm{T}})^{\mathrm{T}}$ consumes a Q'-sized FWHT $P' \cdot K$ times, where P' is due to $\boldsymbol{I}_{P'}$ and K is because $\tilde{\boldsymbol{D}}^{\mathrm{T}}$ has K columns. The number of additions of an Q-sized FWHT is $Q\log_2 Q$ [15]. Thus, we compute the total number of additions as $PMQ\log_2(Q) + P'KQ'\log_2(Q')$ which equals to $N\log_2(QQ')$ due to $PQ = K$, $P'Q' = M$ and $KM = N$. Further, if $\sqrt{QQ'}$ is not a radix-2[3] the normalization requires N multiplications, otherwise it can be achieved with simple bit shifting.

IV. Simulation Results

This section presents the FER performance of the proposed SWH waveform in comparison to OFDM, SC and OTFS. As described in Section II, we consider a quasi-static block fading channel model, i.e., the channel changes among the sub-blocks based on the well known Jakes' model, where a perfect channel estimation is assumed per sub-block. We consider a relative speed between the transmitter and the receiver equal to 300 km/hr with a carrier frequency of 5.9 GHz. The channel power delay profile follows the Extended Vehicular-A (EVA) model, as shown in the Table II. Moreover, due to the satisfactory performance demonstrated in [4], we employ the recursive systematic convolutional encoder with BCJR log-MAP SISO decoder, and the iterative equalization has a maximum of 7 iterations for the spreading waveforms, namely, SC, OTFS and SWH.

[3]By radix-2, we mean the numbers contained in the set $\{1, 2, 4, 8, 16, \cdots\}$.

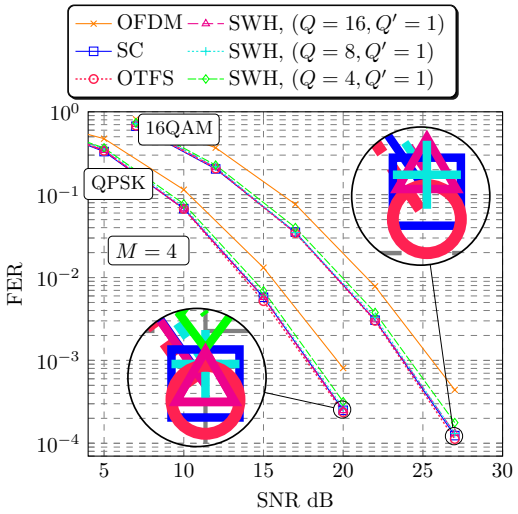

Fig. 2: FER curves $K = 128$, $M = 4$ and $B = 10$MHz.

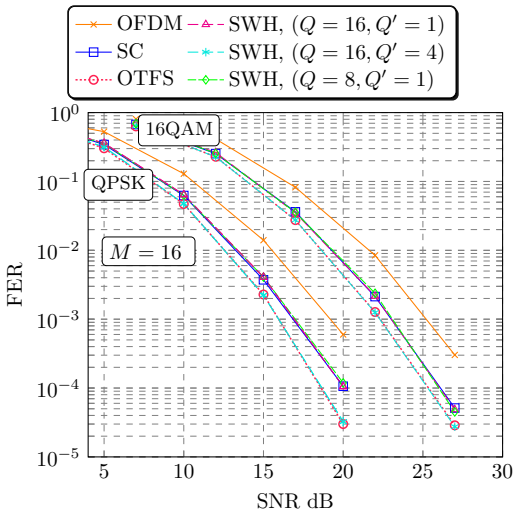

Fig. 3: FER curves $K = 64$, $M = 16$ and $B = 5$MHz.

TABLE II: EVA Channel PDP, delay in μs and power in dB

	1	2	3	4	5	6	7	8	9
μs	0	.03	.15	.31	.37	.71	1.09	1.73	2.51
dB	0	-1.5	-1.4	-3.6	-0.6	-9.1	-7	-12	-16.9

The results presented in Fig. 2 consider $K = 128$, $M = 4$ and a bandwidth of 10 MHz which leads to a channel length of $L = 26$ samples, where we set the CP to 32 samples. In this case, the amount of sub-blocks is not sufficient for the channel to change considerably. For instance, the correlation between the channels of the first and last sub-block is $\mathbb{E}[\tilde{\boldsymbol{h}}_0[\nu]\tilde{\boldsymbol{h}}_{M-1}[\nu]^{\mathrm{H}}] = 0.96$ for any frequency bin ν. This effect can be observed in Fig. 2, since the SC and OTFS present almost the same performance. This indicates, that spread the data among the sub-blocks is not necessary in this case as

TABLE III: Complexity of $\boldsymbol{U}$ for the setups of Figs. 2 and 3

		Fig. 2		Fig. 3	
		Mult.	Add.	Mult.	Add.
SC		1792	3584	3072	6144
OTFS		2304	4608	5120	10240
SWH	$Q=16, Q'=1$	0	2048	0	4096
	$Q=8, Q'=1$	512	1536	1024	3072
	$Q=4, Q'=1$	0	1024	-	-
	$Q=16, Q'=4$	-	-	0	6144

the channel does not significantly change. We compare three configuration of SWH, for $Q = \{16, 8, 4\}$ and $Q' = 1$ for all cases. Notice that $Q' = 1$ means that we do not spread the symbols over the sub-blocks, thus, the performance of SC is the lower-bound, which is a full spreading waveform per sub-block. According to Section III-A, we should have $Q > L = 26$ in order to guarantee the equal gain per sub-block, however, the SWH waveform with $Q = 16$ and 8 have shown very little performance degradation in relation to SC. For SWH with $Q = 4$, the performance loss is more evident, however it has a considerable gain in relation to OFDM.

In Fig. 3, we consider a different setup with $K = 64$, $M = 16$ and bandwidth of 5 MHz which leads to a channel length of $L = 13$ samples, with CP equal to 16 samples. Now the amount of sub-blocks is sufficiently large for the channel to change considerably, which is shown by the correlation $\mathbb{E}[\tilde{\boldsymbol{h}}_0[\nu]\tilde{\boldsymbol{h}}_{M-1}[\nu]^{\mathrm{H}}] = 0.24$ for any ν. Firstly, we notice that the waveforms that localizes the symbols per sub-block experience significant performance loss in relation to OTFS, namely, SC and both SWH systems with $Q' = 1$. This indicates the benefit of spreading the symbols over the sub-blocks. Also, we observe that the SWH with $Q = 16$ and $Q' = 4$ has no performance loss in relation to OTFS, meaning that indeed we can also sparsely spread the symbols over the sub-blocks with no performance loss.

Finally, we show the multiplications and additions of the Table I for the setups of Fig. 2 and Fig. 3. For Fig. 2, we highlight that the smallest configuration of the SWH with $Q = 4$ and $Q' = 1$ has considerable resource savings in relation to SC and OTFS, with little performance loss. For instance, SWH needs no complex multiplication which greatly decreases the overall resource consumption, while SC and OTFS have 1792 and 2304, respectively. For Fig. 3, we give special attention to the configuration $Q = 16$ and $Q' = 4$, which has no performance loss in relation to OTFS and outperforms SC, but has considerable resource savings. In particular, it also requires no complex multiplication.

V. Conclusion

In this letter, we have proposed a robust and low-complexity waveform based on the sparse WHT for doubly-dispersive channels. For the frequency domain sparsity, we have provided a proof for equal gain condition, while we have evaluated numerically the time domain sparsity. In addition, we have presented a general modulation framework, to which the recently proposed OTFS happens to be a particular case. We have shown that both WH and OTFS are robust waveforms due to spreading over time and frequency, however, the proposed sparse WH scheme can be implemented with significantly lower computational complexity.

Appendix

In this appendix, we prove that $\boldsymbol{\Sigma}^{\mathrm{a}}_{\boldsymbol{X}}[n,n] = (\boldsymbol{U}\boldsymbol{\Sigma}^{\mathrm{a}}_{\boldsymbol{d}}\boldsymbol{U}^{\mathrm{H}})[n,n] = \boldsymbol{U}[n,:]\boldsymbol{\Sigma}^{\mathrm{a}}_{\boldsymbol{d}}(\boldsymbol{U}[n,:])^{\mathrm{H}}$ in (12). Because $\boldsymbol{\Sigma}^{\mathrm{a}}_{\boldsymbol{d}}$ is a diagonal matrix, we have the equality

$$\boldsymbol{U}[n,:]\boldsymbol{\Sigma}^{\mathrm{a}}_{\boldsymbol{d}}(\boldsymbol{U}[n,:])^{\mathrm{H}} = \sum_{n'=0}^{N-1} \left|\boldsymbol{U}[n,n']\right|^2 \boldsymbol{\Sigma}^{\mathrm{a}}_{\boldsymbol{d}}[n',n']. \quad (16)$$

In general, $\boldsymbol{U}$ can have zeros if the modulation is sparse, e.g., $\boldsymbol{U}_{\mathrm{SWH}}$ in (11), whose non-zero elements have equal power. Thus, for a fixed row n, we define the set $\chi(n)$ which contains all indexes that have the condition $\boldsymbol{U}[n,n'] \neq 0$. Since $\boldsymbol{U}$ is unitary, $\left|\boldsymbol{U}[n,n']\right|^2 = 1/\left|\chi(n)\right|$, which leads to equation (12).

References

[1] M. Bennis, M. Debbah, and H. V. Poor, "Ultrareliable and Low-Latency Wireless Communication: Tail, Risk, and Scale," *Proceedings of the IEEE*, vol. 106, no. 10, pp. 1834–1853, 2018.

[2] D. W. Matolak, "Channel Modeling for Vehicle-To-Vehicle Communications," *IEEE Commun. Mag.*, vol. 46, no. 5, pp. 76–83, 2008.

[3] G. Miao, N. Himayat, and G. Y. Li, "Energy-efficient link adaptation in frequency-selective channels," *IEEE Trans. Commun.*, vol. 58, no. 2, pp. 545–554, 2010.

[4] R. Bomfin, M. Chafii, and G. Fettweis, "Low-Complexity Iterative Receiver for Orthogonal Chirp Division Multiplexing," in *2019 IEEE Wireless Communications and Networking Conference Workshop (WCNCW)*, 2019, pp. 1–6.

[5] R. Hadani, *et al.*, "Orthogonal time frequency space modulation," in *IEEE WCNC*. IEEE, 2017, pp. 1–6.

[6] R. Bomfin, D. Zhang, M. Matthé, and G. Fettweis, "A Theoretical Framework for Optimizing Multicarrier Systems Under Time and/or Frequency-Selective Channels," *IEEE Commun. Lett.*, vol. 22, no. 11, pp. 2394–2397, 2018.

[7] A. Nimr, M. Chafii, and G. Fettweis, "Precoded-OFDM within GFDM Framework," in *2019 IEEE 89th Vehicular Technology Conference (VTC2019-Spring)*, 2019, pp. 1–5.

[8] K. Beauchamp, *Applications of Walsh and Related Functions, with an Introduction to Sequency Theory*. Academic Press, 1984.

[9] Z. Dlugaszewski and K. Wesolowski, "WHT/OFDM - an improved OFDM transmission method for selective fading channels," in *IEEE Benelux Chapter on Vehicular Technology and Communications. Symposium on Communications and Vehicular Technology. SCVT-2000. Proceedings (Cat. No.00EX465)*, 2000, pp. 144–149.

[10] N. Michailow, L. Mendes, M. Matthé, I. Gaspar, A. Festag, and G. Fettweis, "Robust WHT-GFDM for the Next Generation of Wireless Networks," *IEEE Commun. Lett.*, vol. 19, no. 1, pp. 106–109, 2015.

[11] S. Wang, S. Zhu, and G. Zhang, "A Walsh-Hadamard coded spectral efficient full frequency diversity OFDM system," vol. 58, no. 1, pp. 28–34, 2010.

[12] T. Zemen, M. Hofer, D. Löschenbrand, and C. Pacher, "Iterative Detection for Orthogonal Precoding in Doubly Selective Channels," in *2018 IEEE 29th Annual International Symposium on Personal, Indoor and Mobile Radio Communications (PIMRC)*, 2018, pp. 1–7.

[13] A. Nimr, M. Chafii, M. Matthe, and G. Fettweis, "Extended GFDM Framework: OTFS and GFDM Comparison," in *2018 IEEE Global Communications Conference (GLOBECOM)*, 2018, pp. 1–6.

[14] M. Matthé, D. Zhang, and G. Fettweis, "Low-Complexity Iterative MMSE-PIC Detection for MIMO-GFDM," *IEEE Trans. Commun.*, vol. 66, no. 4, pp. 1467–1480, 2018.

[15] Fino and Algazi, "Unified Matrix Treatment of the Fast Walsh-Hadamard Transform," *IEEE Trans. Comput.*, vol. C-25, no. 11, pp. 1142–1146, 1976.